 doi:10.20944/preprints202208.0521.v1

Article

Exciton-Assisted UV Stimulated Emission with Incoherent Feedback in Polydisperse Crystalline ZnO Powder

Leonid Fedorenko [1,*], Volodymyr Litovchenko [1], Vadym Naumov [1], Dmytro Korbutyak [1], Volodymyr Yukhymchuk[1], Olexander Gudymenko[1], Olexander Dubikovskyi [1], Hidenori Mimura [2] and Arturs Medvids [3]

[1] Lashkaryov Institute of Semiconductor Physics, National Academy of Sciences of Ukraine, Prospect Nauki 41, Kyiv 03028, Ukraine; leonfdrn@gmail.com (L.F.), vadym.naumov@gmail.com (V.N.), dmytro.korbutyak@gmail.com (D.K.), v.yukhymchuk@gmail.com (V.Yu.), gudymen@ukr.net (O.G.), dubikovsky_o@ukr.net (O.D.)

[2] Research Institute of Electronics, Shizuoka University, 3-5-1 Johoku, Naka-ku, Hamamatsu 432-8011, Japan; mimura.hidenori@shizuoka.ac.jp (H.M.)

[3] Institute of Technical Physics, Riga Technical University, Paula Valdena Str. 3/7, Riga LV-1048, Latvia; medvids@latnet.lv (A.M.)

* Correspondence: leonfdrn@gmail.com

Abstract: A comparative analysis of the features of UV- stimulated emission (SE) of various types of disorder active materials based on ZnO crystallites for a random laser (RL) was carried out. The superlinear increase in the intensity of the UV photoluminescence (PL) band of polydisperse nano-microcrystalline (PNMC) ZnO powder at a wavelength of λ = 387 nm and some narrowing of its half-width in the range of 20-15 nm with increasing pump intensity indicate random lasing with incoherent feedback (FB). Properties of similar UV PL bands under the same conditions from a thin film containing hexagonal ZnO microdisks, as well as samples of monodisperse ZnO nanopowder indicate stimulated emission with coherent feedback. It is shown that, among the studied materials, the PNMC ZnO powder with crystallites contained nano-grains with is the most suitable for creating a laser with incoherent feedback at room temperature. The dominant factor of UV SE in PNMC ZnO powder is radiation transitions under exciton - exciton scattering conditions. The possible mechanisms of this random emission with the continuous spectrum are discussed. The average optical gain coefficient α_g at λ = 387 nm in this RL system is estimated, as α_g ~ 150 cm^{-1}.

Keywords: ZnO crystallite; random laser; excitons; stimulated emission; polydisperse powder; thin film; hexagonal microdisks; monodisperse nano-powder; nanophotonics.

1. Introduction

The growing interest in laser-active disorder photonic systems of random lasers (RL) is due, on the one hand, to improve the quality of the light field of stimulated emission (SE), and on the other hand to simplifying and reducing the cost of the microlaser manufacturing. RL is characterized by two types of feedback: coherent or incoherent, and different potential applications, accordingly. The study of the RL is important in fundamental research of the light scattering and amplification in disorder systems and applications in different fields, such as in laser-precise treatment, displays, speckle-free biological imagining [1, 2], surface coding [3], etc. The advantages of RL and the features of its application were fully covered in the reviews [4, 5, 6, 7]. The improvement of the SE light field quality, first of all, is connected with the elimination of the speckles, as optical noise, caused by the coherence nature of the laser radiation. The problem of eliminating or reducing the speckles-negative effect is preferably resolved without the use of super-expensive computers for speckles compensation, especially at fast image changing. The RL with incoherent feedback is the successful decision of speckles elimination based on the nature of SE with the modeless continuous spectrum. The most successful approach was the SE

Preprints (www.preprints.org) | NOT PEER-REVIEWED | Posted: 30 August 2022 doi:10.20944/preprints202208.0521.v1

source based on a disordered medium with strong scattering and high enough photoluminescence (PL) efficiency. One good example of such material became a medium based on ZnO crystallites with extremely high exciton bond energy E_{ex} excitons (~ 60 meV) [8], in which were obtained both coherent [9] as well as incoherent feedback of UV SE, [5] in the microlasers.

Another promising line in the development of microlasers is the use of quasi -2D active media. The latter, especially in the case of ZnO, have a lower lasing threshold due to a developed effective surface, based on exciton lasing at room temperature under optical confinement as compared to 3D [10]. The advantages of the transition from 3D to 2D-like photonic structures are the growth of the surface exciton bond energy Eexs and critical confinement temperature of the e-h system in comparison with the volume [3, 11, 12, 13]. The RL effects were experimentally demonstrated in various quasi-2D structures, including TiO_2 powder colloids [14], and polymer dispersed liquid crystals [15]. Despite the study of a lot of disorder systems with the developed effective surface: Ti-Al_2O_3 powders [16], ZnO powders [4, 7], polycrystalline films [17], fiber lasers [18,19], etc., the influence of excitons, including surface excitons, on the properties and efficiency of such nano- and microsystems has not been sufficiently studied. Perhaps this is related to the long-standing generalization about non-radiative surface defects, which reduce the number of e-h pairs and, accordingly, the quantum efficiency of PL, of course, if we don't take into account the possibility of exciton capture by shallow surface centers.

In this work, we localized attention on the comparative analyses on the influence of ZnO crystallites sizes, shapes, and their distribution in the disordered medium on the UV PL mechanisms, including exciton's contribution from point of view of the dominance of the incoherent SE.

2. Materials and Methods

The samples were prepared in the form of three types of disordered ZnO media: polydisperse nano-micro-crystalline (PNMC) compressed ZnO powder, film-forming solutions, based one-component neutral-curing silicone sealant that cures at room temperature, and microcrystalline hexagonal plate-like films obtained by low-temperature hydrothermal method [20]. PNMC ZnO powder was "white seal", standard BZ0M, declared purity not less than 99.8%, crystal particle size range 50 nm - 2 μm, specific surface area 6-12 m^2/g production of classical chemical and metallurgical French process in a high-temperature Welz furnace. The samples of PNMC ZnO powder were prepared in the form of layers with a thickness of 50 microns sandwiched between quartz plates. For comparison, we also used data for a low-dispersed ZnO powder with nanoparticles (NPs) of an average size of 100 nm, as described in [20]. The experimental setup for laser optical spectroscopic measurements is shown in Figure 1. The PL was excited by the pulsed N2 laser radiation at a wavelength of 337 nm with pulse energy of E = 30 μJ and duration of t_p = 10 ns. The irradiation intensity was controlled by a set of quartz plates and a focusing system. PL spectra were measured by a multichannel optical spectral analyzer (OMA) of the Solar SL40 Duo type equipped with a high-speed 3648-pixel Toshiba CCD detector that provides a sufficiently high spectral resolution and a signal accumulation mode. Emission light from PNMC ZnO powder sample was transmitted by quartz optical fiber to the polychromator entrance slit of OMA. X-ray phase analysis was performed on a Philips X'Pert PRO - MRD diffractometer. Cu Kαl radiation (wavelength λ = 0.15406 nm) was used. The voltage at the anode of the tube was -45 kV, the current -40 mA. The diffractogram was registered in symmetric (2Theta-Omega) mode, the scanning step was equal to 0.025 degrees, and the acquisition time at the point was 1 second. X-ray phase analysis was performed on a Philips X'Pert PRO - MRD diffractometer. CuKα_1 radiation (wavelength λ = 0.15406 nm) was used.

Preprints (www.preprints.org) | NOT PEER-REVIEWED | Posted: 30 August 2022 doi:10.20944/preprints202208.0521.v1

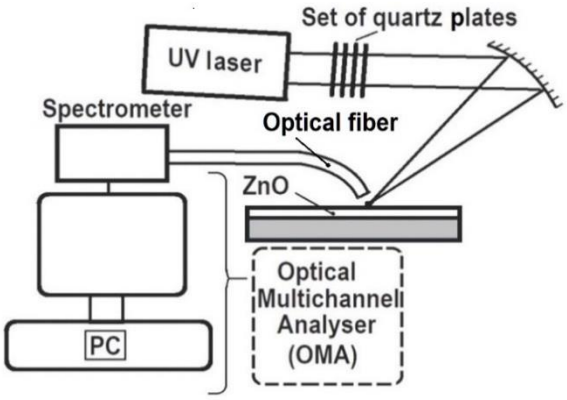

Figure 1. Schematic of optical spectroscopic measurements.

The Raman spectra were excited by the Nd-YAG laser radiation at a wavelength of 532 nm and recorded in the backscattering configuration on a spectrometer, which was a monochromator equipped with an Andor CCD camera. All spectral-optical measurements were carried out at room temperature conditions. The images of the ZnO powder samples' morphology were obtained by the auxiliary scanning electronic microscope (SEM) FESEM, FEI Nova Nano SEM 650.

3. Results and Discussion

The SEM image of the PNMC ZnO cold-pressed samples obtained is shown in Figure 2 a. The constituent elements of the powder are mainly elongated fragments

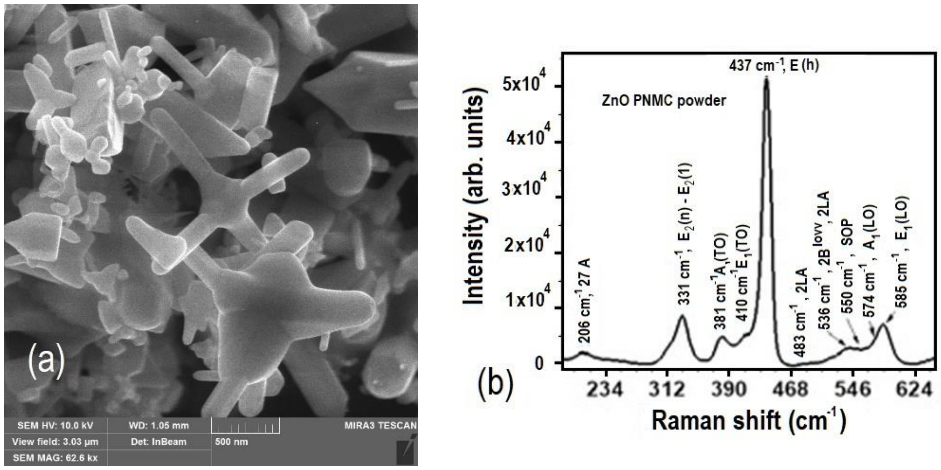

Figure 2. (a) SEM image of morphology of the PNMC ZnO powder after cold pressing; (b) Raman scattering spectrum of the PNMC ZnO powder at room temperature; vibration modes of the first order are marked in bold.

of arbitrary shape, consisting of hexagonal nanocrystallites with a scatter of cross-sectional sizes and lengths in a wide range of 0.05–2 μm.

The Raman scattering spectrum of the PNMC ZnO powder in the region of the first-order vibrational modes is shown in Figure 2 b. Intense Raman bands with a relatively small half-width and the corresponding frequency position indicate that the crystalline phase of wurtzite is inherent in the ZnO nanocrystals. Even though ZnO nanocrystals of different shapes and polycrystals contribute to the Raman spectrum, as can be seen from Figure 2 a, the half-width of the characteristic band with a frequency of 437 cm^{-1} is not significant and is only 13 cm^{-1}. The latter indicates the good crystalline perfection of ZnO nanocrystals. Significantly higher bandwidth with a frequency of 437 cm^{-1} compared to

Preprints (www.preprints.org) | NOT PEER-REVIEWED | Posted: 30 August 2022 doi:10.20944/preprints202208.0521.v1

one with a frequency of 584 cm^{-1}, indicates that the average size of ZnO nanocrystals exceeds 10 nm [21], which correlates well with the data obtained from SEM images.

The diffractogram of the PNMC ZnO powderwas recorded in symmetric (2Θ/ω) mode, the scanning step was 0.025 degrees, and the acquisition time at the point was 1 second. All diffraction peaks on the diffractogram (Figure 3) correspond to the polycrystalline phase of ZnO (PDF 010-74-9939) with parameters a = 3.2494Å; c = 5.2054Å. From the angular positions and values of the half-widths of the reflections (002) and (004) using the Williamson-Hall method, the size of the coherent scattering regions (COS) and the average level of deformations (ε) in the direction of the main optical axis c (ε= 4.8 10^{-4} ; OKR = 25.4 nm.). A similar construction according to reflexes (100) and (200) gives values in the direction of the parameter a (ε= 5.3 10^{-4}; OKR = 26.1 nm). The Williamson-Hall method is based on the graphical method of determining the OCR and ε from construction

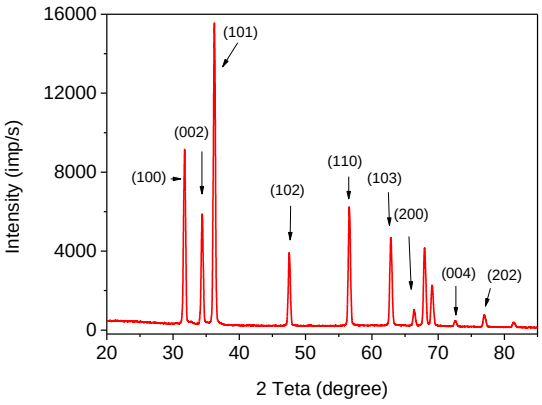

Figure 3. Diffraction pattern of ZnO nanoparticles.

$$\beta\cos\theta = \lambda \backslash D + 4\varepsilon\sin\theta, \quad (1)$$

where β is the half-width of the reflex, θ is the angular position, λ is the wavelength, D is the OCR size, and ε is the average level of deformations. The XRD data correspond well to the conclusions from the Raman shift spectra about the average sizes of ZnO single crystals, as components of larger crystallites, observed in SEM images.

The PL spectra evolution, Figure 4 a), shows the significant growth in the peak

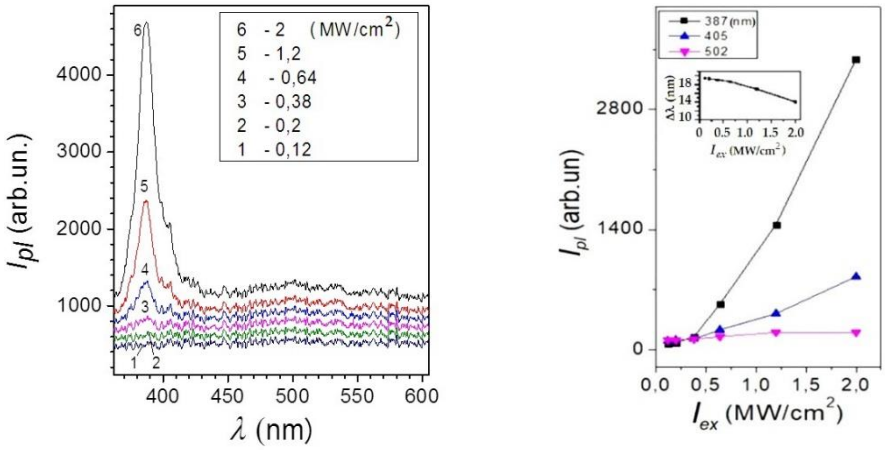

Figure 4. a) Evolution of the PL spectra in the compressed PNMC ZnO powder for different excitation intensities I_{ex} (λ_{ex} = 337 nm) in the range of 0.12 – 2 (MW/cm²) at room temperature. **b)** Dependences of the PL spectral bands intensity I_{pl} versus the excitation intensity I_{ex} (λ_{ex} = 337 nm) for different wavelengths, nm: 387, 405, 502. Insertion: band halfwidth w at 387 nm vs I_{ex}.

Preprints (www.preprints.org) | NOT PEER-REVIEWED | Posted: 30 August 2022 doi:10.20944/preprints202208.0521.v1

intensity I_{pl} of the UV PL band (387 nm) of the PNMC ZnO powder samples with a simultaneous narrowing of its half-width $\Delta\lambda$ (from 19 nm to 14 nm, insert). This indicates the stimulated emission of the UV band contrary to the visible bands: 405 nm (C - V_{Zn}), 502 nm (V_O), 544 nm (O_i) [7] with weak increasing, and spontaneous emission, Figure 4 b). The spectral position of the peak (405 nm) coincides with the position of the e–h plasma PL band at high excitation intensity Iex for the single crystalline ZnO film, obtained by MBE [21]. Nevertheless, the 405 nm peak for PNMC ZnO powder does not shift at all I_{ex} levels. Besides, it is considerably narrower ($\Delta\lambda \leqslant 2$ nm) as compared to e-h plasma band ($\Delta\lambda \approx 8$ nm) shifted in case of the excitons decay and renormalization of the band gap. These circumstances indicate a high probability of the excitonic nature of the transmission in UV PL band (387 nm). Lasing at a wavelength of 387 nm occurs in the so-called diffusion mode due to the incoherent or "energy" FB [22]. In this case, adjacent modes spectrally overlap, which gives a continuous spectrum of emission. This result qualitatively differs from observations on the samples of the ZnO film with hexagonal microdisks formed by the method based on a low-temperature solution [20].

Hexagonal ZnO microdisks had a distribution with some disordered orientation in space and size variation Figure 6 c [23]. In this case, the PL spectrum occurs with a comb-like

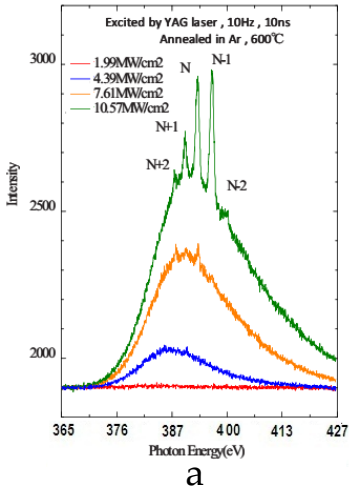

a

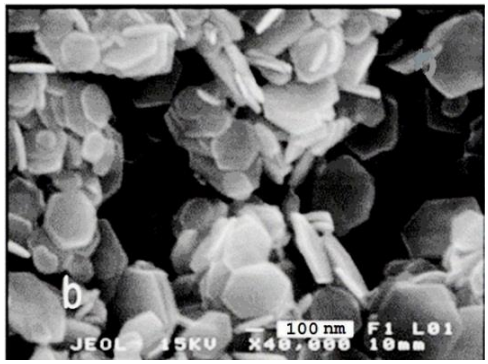

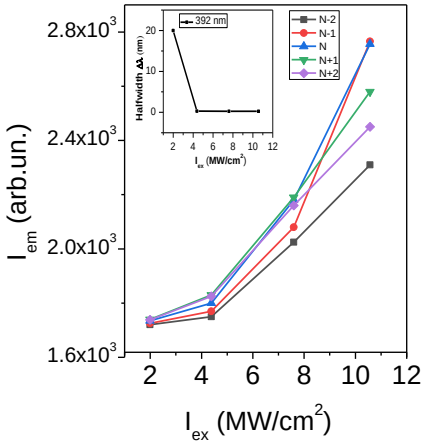

c

Figure 5. a) UV PL spectra evolution on the intensity of excitation I_{ex} (λ=355 nm) for the ZnO film with hexagonal microdisks;
b) SEM images of the ZnO film containing the hexagonal microdisks;
c) the PL ultranarrow peacks intensity versus I_{ex} at the wavelengths λ_{PL} (nm) = 388, 391, 392, 397, 399, constructed according to [23] for comparison; Insert: the UV PL spectral band halfwidth versus the I_{ex}, N is mode number.
The data from [23] were used with permission

regular arrangement of ultra-narrow bands (peaks) with halfwidth $\Delta\lambda$ ~ 0.25 nm. Superlinear growth of I_{Pl} in the range of excitation intensities I_{ex} indicates the presence of

Preprints (www.preprints.org) | NOT PEER-REVIEWED | Posted: 30 August 2022 doi:10.20944/preprints202208.0521.v1

coherent or "amplitude" FB [17]. Stimulated emission has a mode composition formed by whispering gallery modes (WGM) formed inside (on the faces) of hexagonal microdisks. It is noteworthy that the threshold of stimulated emission, in this case, coincides with the appearance of the comb of narrow peaks that confirms the unrandom nature of the ultranarrow peacks appearance.

A fundamentally different character of the evolution of PL spectra was observed in

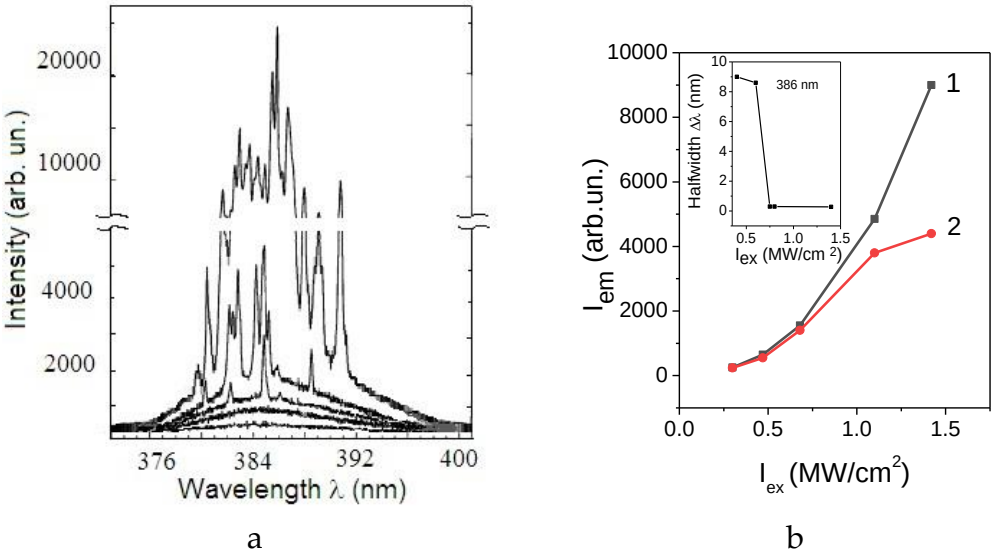

Figure 6. a) - UV PL spectra evolution of the monodispersed ZnO powder under excitation intensity in the range (from bottom to top): 400, 562, 763, 875, and 1387 kW/cm^2 (taken from reference [8] with permission). The size on the ZnO crystallite is equal 100 nm;
b) Dependencies of UV PL I_{em}: (1) – the spectral-integral intensity of UV-PL emission; (2) – dependence of a separate ultra-narrow peak (386 nm) from monodisperse ZnO powder on the excitation intensity I_{ex}; inset: mean half-width of UV PL peaks as a function of I_{ex}. (constructed from reference [8] with permission).

nanopowder with one-dimensional NPs size distribution, with an average size ~ 100 nm with strong scattering, Figure 6, [8]. The ultra-narrow bands (0.2 nm) in PL spectra appeared in a chaotic sequence with irregular spectral intervals, unlike [23]. This is associated with the stochastic nature of the resonator loop formation in the excited volume. SE, in this case, may arise initially as a result of incoherent amplification regardless of the appearance of ultra-narrow peaks. Their occurrence does not coincide with the SE threshold, since the coherent ultra-narrow peaks arise according to the stochastic formation of a closed photon track. The superlinear growth of the UV band PL intensity I_{em} in the spectra of PNMC ZnO powder shown in Figures 4 on the pump intensity I_{ex}, is qualitatively similar to the data of the film with ZnO hexagonal microdisks (Figure 5) [23] and to the integral spectrum intensity in the powder containing the NPs ZnO with an average particle size of 100 nm (Figure 6, curve 1) [8]. There is a tendency to sublinearity for a single ultra-narrow peak (386 nm) at the end of curve 2 (Figure 6), which can be explained by the redistribution of the SE energy on emerging random modes.

The conditions for the absence of the ultra-narrow peak in the disordered laser medium can be evaluated from the threshold criterion expression for the critical volume of V_{cr} [23]:

$$V_{cr} \approx (l_t \cdot l_g / 3)^{3/2}, \quad (2)$$

Preprints (www.preprints.org) | NOT PEER-REVIEWED | Posted: 30 August 2022 doi:10.20944/preprints202208.0521.v1

where l_g - is the length of the gain in the scattering medium, l_t - the free path of the photon, at which the direction of its motion becomes unpredictable (there is a "randomization" direction)

$$l_t = l_s/(1-\cos\theta), \quad (3)$$

where ls is the path between the two scattering acts, θ is the scattering angle.

Given the spectrum evolution of the central UV spectral band (λ_{max} = 387 nm) of PNMC ZnO powder, allows to be concluded that the photon transport occurs in the so-called "diffusion mode"($L >> l_t >> \lambda$), where L is the characteristic size of random media) within the critical excitation volume $V_{ex} < V_{cr}$. The significant dispersion of particle sizes (0.05 – 2 μм) and shapes in PNMC ZnO powder (Figure 2 a), complicates software processing data for their averaging. Therefore, in the estimations of the effective gain length [4]:

$$l_{amp} = \sqrt{\frac{l_t \times l_g}{3}}, \quad (4)$$

we will limit ourselves to the probable range of l_t and l_g from the condition that $V_{ex} \le V_{cr}$, according to relation (1). We take into account that the size of laser spot $d_{ex} \approx 20$ μm and excited layer thick $d_l > 10$ μm, and also that only from 1 to 5% of the exciting light is absorbed by ZnO nanopowder, rest is scattering [4]. This corresponds to a depth of absorption from $7.14 \cdot 10^{-5}$ cm ($\alpha = 1.4 \cdot 10^{4}$ cm^{-1}) to $3.6 \cdot 10^{-4}$ cm ($\alpha = 2.8 \cdot 10^{3}$ cm^{-1}) at the wavelength of the nitrogen laser (λ = 337 nm), where α is the absorption coefficient. Then the value range of the exciting volume is about $V_{ex} = 3.0 \cdot 10^{-8} \div 1.0 \cdot 10^{-7}$ cm^3. The probable range of values of the critical volume of the SE source depending on the gaine length l_g and length of randomization l_t is shown on Figure 7. The range of the gain path of lengths l_g is from $5 \cdot 10^{-2}$ to 10^{-1} cm, provided that the range of lengths of «randomization» l_t of the motion direction of the photon is determined within $l_t = 10^{-3} \div 10^{-2}$ cm. Obtained gain factor $(l_g)^{-1} = 20 \div 10$ cm^{-1} were not too high. But the gain effect between the start and endpoints of the full length of the gain path l_g [4] is l_{amp} = 0.0041-0.018 cm, which corresponds to the average value of the gain $(l_{amp})^{-1}$ = 150 cm^{-1}.

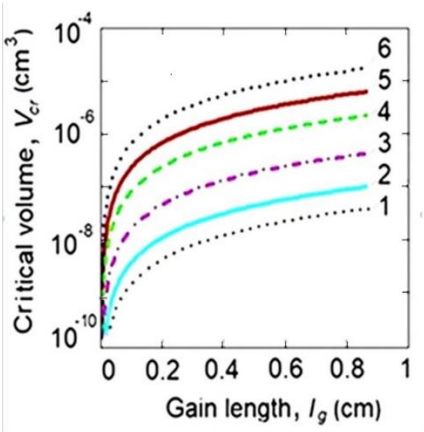

Figure 7. Dependences of the critical volume Vcr on the gain length lg at different average randomized lengths lt, μm: 1 - 0.387 (1λ); 2 – 0.74 (2λ); 3 –1.94 (3λ); 4 – 5.85 (15λ); 5 – 11.6 (30λ); 6 – 15.5 (40λ).

It should be noted that in all modifications of PNMC of ZnO powder, the effect of incoherent FB is implemented. The photon transport occurs in the so-called "diffusion mode" within the critical excitation volume $V < V_{cr}$. This allows keeping SE in the incoherent mode at all ranges of excitation by using nitrogen laser N_2. The position of the UV band maximum at 387 nm fixed at all pumping levels of the PNMC ZnO powder coincides with the maximum of the so-called "P" exciton band in single-crystal ZnO films [22]. This is responsible for exciton stimulated emission under conditions of inelastic exciton-exciton

Preprints (www.preprints.org) | NOT PEER-REVIEWED | Posted: 30 August 2022 doi:10.20944/preprints202208.0521.v1

scattering [24, 25]. Its fixed spectral position with increasing I_{ex} in our case is caused by an increase of the excitons concentration n_{ex}, preventing them from breaking up and transitioning into e-h plasma (with a shift of the maximum to λ ~ 405 nm). We consider two possible explanations: 1) due to the giant oscillator strength f_{NPex} [26]:

$$f_{NPex} \cong \frac{3}{4}\left|\frac{a_B^*}{R}\right|^3 f_{Bex}, \quad (5)$$

(where f_{Bex} is the oscillator strength in the crystal bulk, a^*_B is Bohr radius of the exciton, R is the NP's radius) at the condition that the crystal size is larger than the exciton Bohr radius (a^*_B ~ 2 nm) but smaller than the optical wavelength (387 nm) [22].

2) increase of the binding energy of excitons E_{ex} and, accordingly, their concentration n_{ex}. It can be assumed that the surface capture centers of excitons existing at the interface of nanocrystals (between grains of ~25 nm) as parts of larger ZnO particles, recorded on the SEM image, Figure 2a, are responsible for the growth of E_{ex}. The increase of n_{ex} leads to an increase in the exciton self-scattering and SE in the PNMC ZnO. Thus, the interfaces between nanocrystals can be considered as barriers that lead to the excitons confinement in nanocrystal grains (~25 nm in size). We plan to study the peculiarities of the kinetics of exciton transitions in PNMC ZnO powder under these conditions in the near future.

Summarizing the above, we can conclude that to improve the stimulated modeless emission efficiency of such a multi-element system, it is advisable to take into account and use the influence of the effective surface. The latter appears very developed due to a large number of nanocrystal surfaces that can significantly increase the concentration of the exciton capture centers without an increase of the light scattering. This aspect has not been given due attention in previous studies, including those cited in the text. The surface plays a dominant role in such multi-element systems due to several important factors: exciton capture in shallow surface centers, quantum confinement effect in 2D-like platelet nanosystems, mirror reflection forces, and correlation forces, which under certain conditions lead to an increase in E_{ex} and, accordingly, exciton inversion population (see, for example, [11]). Clarification and confirmation of the priority of the specified mechanisms is expected in our further studies.

4. Conclusions

A comparative analysis of the optical spectral and structural properties among various types of crystallites ZnO structures allowed us to establish:

1. Among considered crystalline ZnO systems the polydisperse nano- microcrystalline (PNMC) powder with a ZnO particle size ranging from 50 nm to 2 μm showed the random UV SE (λ = 387 nm) with incoherent feedback in all ranges of excitation intensity.
2. The dominant factor for UV SE at λ = 387 nm in the PNMC ZnO powder at room temperature is exciton-exciton scattering-assisted radiative transitions;
3. The average value of the optical gain at λ = 387 nm in the PNMC ZnO powder RL is estimated to be as high as 150 cm^{-1}.
4. ZnO thin film with hexagonal microdisks as well as low-dispersed ZnO nanopowder demonstrate UV SE with coherent feedback and ultra-narrow spectral peaks: regular

in the case of the hexagonal microdisks, and irregular in the case of monodisperse ZnO powder with a particle size of ~ 100 nm, accordingly.

Author Contributions: Conceptualization, L.F., V.L., and H.M.; methodology, L.F., V.N., V.Yu. and A.M.; validation, L.F., V.N. and V.Yu.; formal analysis, L.F., D.K. and H.M.; investigation, L.F., V.N., V.Yu., O.G., O.D., A.M., and H.M.; resources, D.K., and A.M.; data curation, L.F., V.N., and V.Yu.; writing—original draft preparation, L.F., and A.M.; writing—review and editing, L.F., V.N., V.Yu., and A.M., visualization, L.F., V.N., and A.M.; supervision, L.F., and D.K. All authors have read and agreed to the published version of the manuscript.

Funding: This research received no external funding but was supported by ongoing research programs of the National Academy of Sciences of Ukraine and of the Riga Technical University, Latvia, Project N 14508.

Data Availability Statement: The data that support the findings of this study are available from the corresponding author upon reasonable requests.

Acknowledgments: This work was performed due to the scientific cooperation between the Lashkaryov Institute of Semiconductor Physics, National Academy of Sciences of Ukraine, the Institute of Technical Physics, Riga Technical University, and the Research Institute of Electronics, Shizuoka University. The authors thank Professor Hui Cao, head of the Research Laboratory at Yale University, the USA for kindly granting permission to use the experimental data for comparison calculations.

Conflicts of Interest: The authors declare no conflict of interest.

1. Song, Q.; Xu, Z.; Choi, S. H.; Sun, X.;, Xiao S.; Akkus, O.; and Kim, Y. L. Detection of nanoscale structural changes in bone using random lasers. *Biomedical Optics Express.* **2010,** *11,* 1401**-** 1407, https://doi.org/10.1364/BOE.1.001401
2. De Armas-Rillo S.; Fumagallo-Reading F.; Luis-Ravelo D.; Abdul-Jalbar B.; González-Hernández T. and Lahoz F. Random Lasing Detection of Mutant Huntingtin Expression in Cells. *Sensors (MDPI)* **2021**, *21(11)*, 3825, https://doi.org/10.3390/s21113825.
3 Wiersma, D.S. The physics and applications of random lasers. *Nature Phys.* **2008**, *4,* 359-367, https://doi.org/10.1038/nphys971.
4. Cao H. Lasing in random media. *Topical Review Waves Random Media.* **2003**, *13,* R1–R39, https://doi.org/10.1088/0959-7174/13/3/201.
5. Cao, H.; Chriki, R.; Bittner, S.; Friesem, A.A.; Davidson, N. Complex lasers with controllable coherence. *Nat. Rev. Phys.* **2019,** *1,* 156-168, https://doi.org/10.1038/s42254-018-0010-6.
6. Noginov, M.A. Lasers with Nonresonant Feedback and Laserlike Emission from Powders: Early Ideas and Experiments. *Solid-State Random Lasers*. [Springer Series in Optical Sciences] Springer, NY, USA. 2005; (Chapter 1), pp. 1-9, doi:10.1007/0-387-25105-7_1.
7. Lu, Y.J.; Shi, Z.F.; Shan, C.X.; Shen, D.Z. ZnO nanostructures and lasers. In *Nanoscale Semiconductor Lasers. Micro and Nano Technologies;* Tong, C., Jagadish, C., Eds.; Elsevier: Amsterdam, Netherlands, **2019**; Chapter 4, pp. 75-108, https://doi.org/10.1016/B978-0-12-814162-5.00004-2.

8. Cao, H.; Zhao, Y.G.; Ho, S.T.; Seelig, E.W.; Wang, Q.H.; Chang, R.P.H. Random laser action in semiconductor powder. *Phys. Rev. Lett*. **1999**, 82, 2278-2281, https://doi.org/10.1103/PhysRevLett.82.2278.
9. Thareja, R.K.; Mitra A. Random laser action in ZnO. *Appl. Phys. B, Lasers and Optics*. **2000**. *B 71*, 181–184, DOI: 10.1007/s003400000274.
10. Ye, Y.; Wong, Z.J.; Lu, X.; Ni, X.; Zhu, H.; Chen, X.; Wang, Y.; Zhang, X. Monolayer excitonic laser. *Nat. Photonics* **2015**, *9*, 733-737, https://doi.org/10.1038/nphoton.2015.197.
11. Lytovchenko, V.G.; Fedorenko, L.L.; Korbutyak, D.V.; Strikha, M.V. Ordered electron-hole condensate as a perspective 2D laser environment at room temperatures. *Ukr. J. Phys.* **2021**, *66*, 612-617, DOI: https://doi.org/10.15407/ujpe66.7.612.
12. Litovchenko, V.G.; Korbutyak, D.V.; Kryuchenko, Yu.V. Investigation of the collective properties of excitons in polar semiconductors (ZnO). *Sov. Phys. JETP*. **1981**, *54*, 1093-1099.
13. Korbutyak, D.V.; Litovchenko, V.G. Electron-hole condensate in semiconductors with high exciton energy. *Sov. Phys. Solid State*. **1981,** *23*, 1411-1416.
14. Lawandy, N.M.; Balachandran, R.M.; Gomes, A.S.L.; Sauvain, E. Laser action in strongly scattering media. *Nature* **1994**, *368*, 436-438, https://doi.org/10.1038/368436a0
15. Stefano Gottardo, Stefano Cavalieri, Oleg Yaroshchuk, and Diederik S. Wiersma. Quasi-Two-Dimensional Diffusive Random Laser Action. *Phys.Rev.Let.* **2004,** *93*, 263901-1-263901-4, https://doi.org/10.1103/PhysRevLett.93.263901
16. Wiersma, D.S.; van Albada, M.P.; Lagendijk, A. Coherent backscattering of light amplifying random media. *Phys. Rev. Lett.* **1995,** *75*, 1739-1742. DOI: 10.1103/PhysRevLett.75.1739.
17. Cao, H.; Xu, J.Y; Zhang, D.Z.; Chang, S.-H.; Ho, S.T.; Seelig, E.W.; Liu, X.; Chang; R.P.H. Spatial confinement of laser light in active random media. *Phys. Rev. Lett.* **2000**, *84*, 5584-5587, https://doi.org/10.1103/PhysRevLett.84.5584.
18. Gomes, A.S.L.; Moura, A.L.; de Araújo, C.B.; Raposo, E.P. Recent advances and applications of random lasers and random fiber lasers. *Prog. Quantum Electron.* **2021**, *78*, 100343,1-69, https://doi.org/10.1016/j.pquantelec.2021.100343.
19. Wiersma, D.S. Disordered photonics. Nat. Photonics 2013, 7, 188-196. DOI: 10.1038/NPHOTON.2013.29.
20. Han, G.; Okada, M.; Xiao, Z.Y.; Neo, Y.; Aoki, T.; Mimura, H. Cathodoluminescence of single disk-like ZnO prepared by the low-temperature solution-based method. *e-J. Surf. Sci. Nanotech*. **2009**, *7*, 354-357, DOI: 10.1380/ejssnt.2009.358.
21. Ohtomo, A., Kawasaki M., Sakurai Y., Yoshida Y., Koinuma H., Yu P., Tang Z.K., Wong G.K.L., Segawa Y. Room temperature ultraviolet laser emission from ZnO nanocrystal thin films grown by laser MBE. *Materials Science and Engineering*. **1998**, *B54*, 24–28. https://doi.org/10.1016/S0921-5107(98)00120-2.
22. Cao, H. Lasing in random media. *Waves Random Media.* Publisher: Taylor & Francis, London, UK, **2003**, *13*, R1–R39, https://doi.org/10.1088/0959-7174/13/3/201.
23. Han, G.; Shibukawa, A.; Okada, M.; Neo, Y.; Aoki, T.; Mimura, H. Nanosized hexagonal plateletlike ZnO for nanophosphor applications. *J. Vac. Sci. Technol. B*. **2010**, *28*, C2C16-C2C19, doi: 10.1116/1.3292573.
24. Bagnall, D. M.; Chen, Y. F.; Zhu, Z.; Yao, T.; Shen, M. Y.; Goto, T. High temperature excitonic stimulated emission from ZnO epitaxial layers. *Appl. Phys. Lett.* **1998,** *73*, 1038-1040, http://dx.doi.org/10.1063/1.122077.
25. C. Klingshirn. The Luminescence of ZnO under High One- and Two-Quantum Excitation. *Phys. Stat. Sol. (B).* **I975,** *71*, 547-556, doi: 10.1002/pssb.2220710216.
26. Kayanuma, Y. Quantum-size effects of interacting electrons and holes in semiconductor microcrystals with spherical shape. *Phys. Rev. B.* **1988**, *38*, 9797-9805, doi:10.1103/PhysRevB.38.9797.